ROCK ABRASION TEXTURES ALONG CURIOSITY'S TRAVERSE

N.T.Bridges[1], F.J. Calef[2], B. Hallet[3], K.E. Herkenhoff[4], N.L. Lanza[5], S. Le Mouélic[6], C.E. Newman[7], D.L. Blaney[2], M.A. de Pablo[8], G.A. Kocurek[9], Y. Langevin[10], K.W. Lewis[11], N. Mangold[6], S. Maurice[12], P.-Y. Meslin[12], H.E. Newsom[13], P. Pinet[12], N.O. Renno[14], M.S. Rice[15], M.E. Richardson[7], V. Sautter[16], R.S. Sletten[3], R.C. Wiens[5], and R.A. Yingst[17]; [1]Applied Physics Laboratory, Laurel, MD 20723; [2]Jet Propulsion Laboratory, Pasadena, CA 91109; [3]University of Washington, Seattle, WA 98195-1310; [4]U.S. Geological Survey, Flagstaff, AZ 86001; [5]Los Alamos National Laboratory, Los Alamos, NM 87545; [6]LPGNantes, UMR 6112, CNRS/Université de Nantes, Nantes, France; [7]Ashima Research, Pasadena, CA 91106; [8]Universidad de Alcala, 28871 Madrid, Spain; [9]University of Texas, Austin, TX 78712; [10]Institute d'Astrophysique Spatiale, Université Paris-Sud, Orsay, France; [11]Princeton University, Princeton, NJ 08544;[12]CNRS-Université Toulouse, 31400 Toulouse, France; [13]University of New Mexico, Albuquerque, NM 87131-0001; [14]University of Michigan, Ann Arbor, MI 48109-2143; [15]California Institute of Technology, Pasadena, CA 91125; [16]Lab Mineral and Cosmochim Museum, F-75005 Paris, France; [17]Planetary Science Institute, Tucson, AZ 85719-2395

Introduction

Mars is a dry planet, with actively blowing sand in many regions [1-5]. In the absence of stable liquid water and an active hydrosphere, rates of chemical weathering are slow, such that aeolian abrasion is a dominant agent of landscape modification where sand is present and winds above threshold occur at sufficient frequency. Reflecting this activity, ventifacts, rocks that have been abraded by windborne particles, are common on the Martian surface. They provide invaluable markers of the Martian wind record and insight into climate and landscape modification. The Mars Science Laboratory (MSL) "Curiosity" payload is well suited for studying ventifacts and modern wind patterns which are relevant for understanding current abrasion conditions. The rover mast cameras, Navcam, Mastcam, and the ChemCam Remote Micro Imager (RMI) provide images of varying coverage and spatial scale. In particular, the Mastcam M100 (right eye) and ChemCam Remote Micro Imager (RMI), with pixel scales 74 [6] and 19.6 μrad [7-8], provide fine details of rock textures.

Methods

Ventifacts were identified in systematic searches through all M100, RMI, and MAHLI images, the three datasets with the highest spatial resolution. Diagnostic characteristics were tabulated for each ventifact, including 1) overall shape (facet, keel, basal sill), 2) macro-texture (elongated pits, scallops, flutes, grooves, and rock tails) and 3) micro-texture (lineations). Once found, rocks were located in the lower resolution Navcam data, such that the location, size (height and width), and orientation of most ventifacts could be computed using Navcam stereo mosaics in the Mars Science Laboratory InterfaCE (MSLICE) software package available to the MSL Team [9,10]. The ventifact locations were projected onto the color portion of an orthorectified High Resolution Imaging Science Experiment (HiRISE) image with an overlain rover traverse path and sol location markers (Fig. 1). The orientations were also compiled into rose diagrams and, following past convention [11,12], shown as a function of upwind direction. The MarsWRF atmospheric model [13-14] was used to predict the present day wind field at the MSL landing site.

Results

Ventifacts are found throughout the traverse (Fig. 1-3). The ventifacts contain one or more diagnostic features and textures: Facets, keels, basal sills, elongated pits, scallops/flutes, grooves, rock tails, and lineations (Fig. 3). Wherever a range of imaging scales is available for the ventifacts, the highest resolution data, generally from RMI and MAHLI, consistently show evidence for abrasion in the form of micro-scale lineations. From Bradbury to Rocknest, the rose diagram of ventifact-derived wind azimuths shows inferred winds from all 30° bins, but with a strong bias to westerly flow (38 measurements, or 79% percent of sample), with the strongest trend in the 210-240° bin (Fig. 4**)**. Predicted winds at the grid point closet to the MSL landing site (137.444°E, 4.55°S) shows a poor correlation to these results. Studies of dune and ripple orientations and displacement in the barchans field southwest of the MSL landing site indicate strong bidirectional winds from the NW and ENE, with mesoscale modeling in the same paper indicating a dominance of ENE winds in the dunefield [15]. Similarly, the direction of scarp retreat and rock tails in Yellowknife Bay to the northeast of Rocknest is consistent with northeasterly winds that, based on cosmic ray exposure ages, occurred 78±30 Ma [16]. The ventifact trends that require a predominance of northwesterly-southwesterly flow are not predicted by the wind models, ENE bedform orientations, and Yellowknife results, but are consistent with the NW bedform orientations.

Discussion

Ventifacts are distributed throughout the traverse, which includes those near the indurated (inactive) coarse grain-coated Rocknest sand shadow [17-18] and areas lacking any sand deposits. Some rocks, such as Jake, a large (~half a meter) rock in a sand-free area, have basal sills indicative of soil deflation. This indicates that fine, loose particles have been removed from this region, leaving behind remnant rocks and indurated bedforms. Evidence for deflation is consistent with the burial and exhumation hypothesis.

Other ventifacts, such as Slide Mountain (Fig. 3), have basal undercuts indicating sand abrasion near the surface.

HiRISE images do not show any dark sand dunes in the traverse so far, in contrast to the large dune field ~2.6 km to the south that shows evidence for current migration by winds from the NW and ENE [15]. Because significant rock abrasion requires the presence of saltating sand [19], these observations suggest that ventifact formation occurred during periods in the past when sand was more plentiful locally. One possibility is that sand migration pathways have varied over time. Alternatively, a fresh supply of sand could have been delivered by the Peace Vallis alluvial fan whose margin is near this area [20]. This supply-limited sand source would abrade rocks before subsequently becoming depleted or indurated. The ventifact-derived westerly wind vectors detected in the first 100 sols may be from rare winds not predicted by models, perhaps in a past epoch.

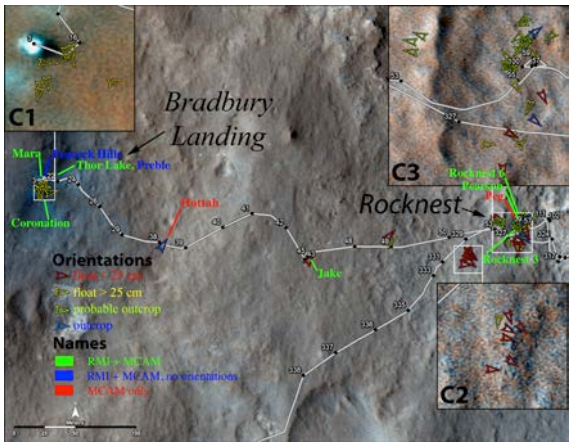

Figure 1: Curiosity's traverse through Sol 338 overlaid on a HiRISE color strip. The white numbering shows the rover position as a function of sol. Arrows point toward the inferred downwind ventifact directions. Three enlargement of ventifact clusters (C1, C2, and C3) are shown.

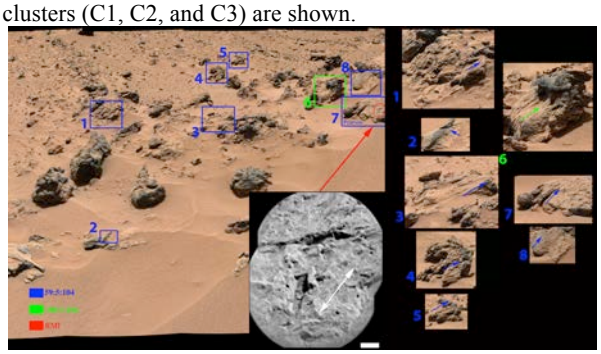

Figure 2: Portion of Mastcam left mosaic mcam00296 showing ventifacts in the Rocknest region that encompass ventifact Cluster 3. Blue and green boxes reference the Navcam mosaic used to derive inferred wind orientations. These are enlarged at right, with the arrows pointing in the inferred downwind direction. The red outline shows the location of the RMI mosaic of Pearson, at lower right. Scale bar is 1 cm.

Figure 3: Mastcam M100 image (mcam01715) of Slide Mountain rock, which has been undercut, probably be wind, on its SW-facing side.

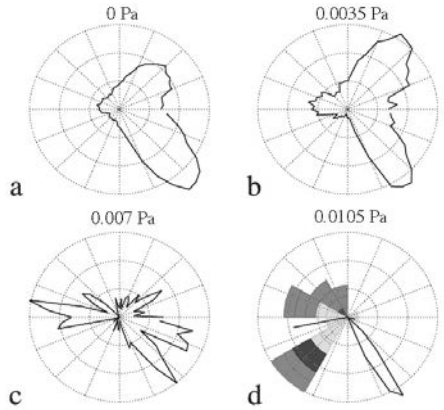

Figure 4: Relative fractions of predicted wind shear stresses above the given shear stress over a Mars year shown as upwind azimuth. The location is centered on the MSL landing site (137.444°E, 4.55°S), with a resolution of ~4 km. The upwind directions indicated by large float and bedrock ventifacts is overlaid on 4c in order to compare the rock record with the wind predictions.

References [1] Silvestro, S. et al. (2010), *GRL 37*, doi:10.1029/2010GL044743. [2] Chojnacki et al. (2011), *JGR, 116*, doi:10.1029/2010JE003675. [3] Hansen, C.J. et al. (2012), *Science, 331*, 575-578. [4] Bridges et al. (2012*a*), *Geology, 40,* 31-34. [5] Bridges et al. (2012*b*), *Nature, 485*, 339-342. [6] Malin, M.C. et al. (2010), *Lun. Planet. Sci. XLI*, 1123. [7] Maurice, S. et al. (2012), *Space Sci. Rev.*, doi: 10.1007/s11214-012-9912-2. [8] Le Mouélic, S. et al. (2014), *Icarus*, in press. [9] Aghevli, A. et al. (2006), *5th International Workshop on Planning and Scheduling for Space*. [10] Crockett, T. et al. (2006), IEEECA paper #1489. [11] Laity, J.E. (1994), Landforms of aeolian erosion; in Abrahams, A. D. and A.J. Parsons (eds), *Geomorphology of Desert Environments,* Chapman and Hall, London, 506–535. [12] Bridges, N.T. et al. (2004), *Planet. Space Sci., 52*, 199-213. [13] Richardson, M.I. et al. (2007), *JGR, 112*, doi: 10.1029/2006JE002825. [14] Toigo, A.D. (2012), *Icarus, 221*, 276-288, [15] Silvestro, S. et al. (2012), *Geology, 41*, 483-486. [16] Farley, K.A. et al. (2014), *Science, 343*, 1247166. [17] Goetz, W. et al. (2013), *Lun. Planet. Sci. XLIV*, 1222. [18] Kocurek, G. et al. (2013), *Lun. Planet. Sci. XLIV*, 1375. [19] Laity, J.E.and N.T. Bridges (2009), *Geomorphology, 105*, 202-217. [20] Palucis, M.C. et al. (2013), *Lun. Planet. Sci. XLIV*, 1607.